

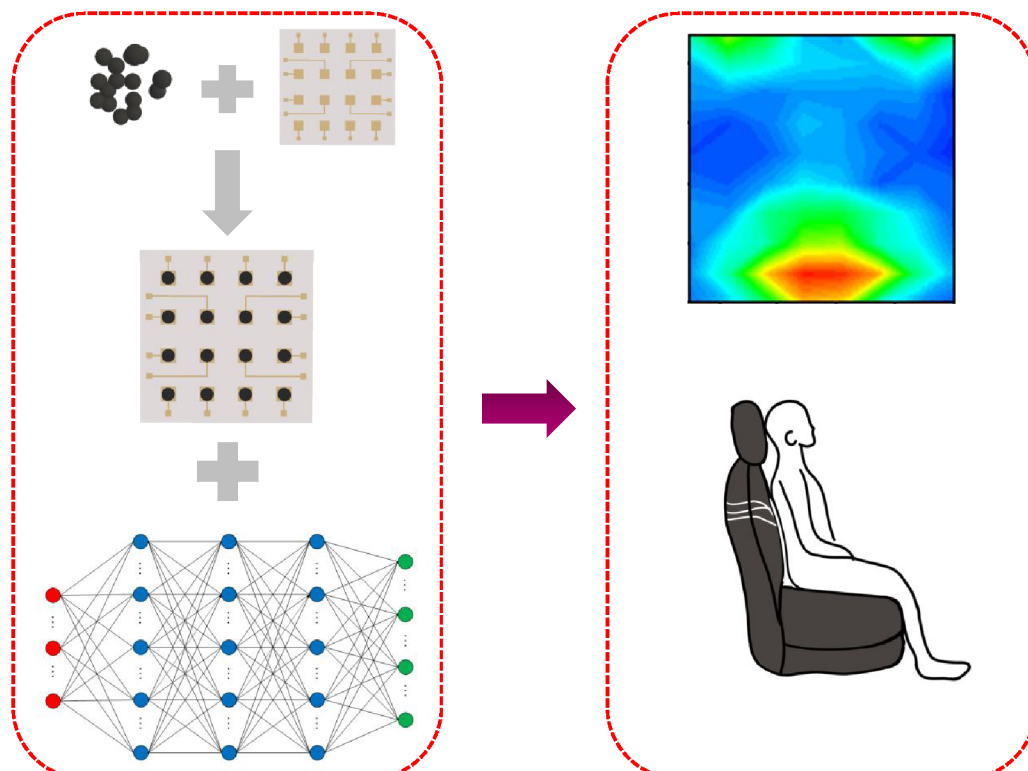
Large-area flexible MWCNTs/PDMS pressure sensor for ergonomic design with aid of deep learning

Journal:	<i>IEEE Sensors Journal</i>
Manuscript ID	Sensors-43561-2021
Manuscript Type:	Regular Paper
Date Submitted by the Author:	01-Sep-2021
Complete List of Authors:	Zhong, Hongchuan Fu, Rongda Chen, Nuo Chen, Shiqi Zhou, Zaiwei Zhang, Yue Yin, Xiangyu He, Bingwei
Keywords:	MECH

SCHOLARONE™
Manuscripts

Large-area flexible MWCNTs/PDMS pressure sensor for ergonomic design with aid of deep learning

Graphic abstract :



Large-area flexible MWCNTs/PDMS pressure sensor for ergonomic design with aid of deep learning

Hongchuan Zhong^{‡a}, Rongda Fu^{‡a}, Nuo Chen^{‡b}, Shiqi Chen^a, Zaiwei Zhou^a, Yue Zhang^{a,c,*}, Xiangyu Yin^{c,d*}, Bingwei He^{a,b}

a. College of Mechanical Engineering and Automation, Fuzhou University, Fuzhou 350108, China

b. Department of Mechanical and Energy Engineering, Southern University of Science and Technology, Shenzhen 518055, China

c. Fujian Engineering Research Center of Joint Intelligent Medical Engineering, Fuzhou 350108, China

d. College of Chemical Engineering, Fuzhou University, Fuzhou 350108, China

‡ Hongchuan Zhong, Rongda Fu and Nuo Chen contributed equally to this work.

*Corresponding authors: Yue Zhang (yuezhang@fzu.edu.cn); Xiangyu Yin (xyin65@fzu.edu.cn)

Abstract: The achievement of well-performing pressure sensors with low pressure detection, high sensitivity, large-scale integration and effective analysis of the subsequent data remains a major challenge in the development of flexible piezoresistive sensors. In this paper, a simple and extendable sensor preparation strategy was proposed to fabricate haptic sensors based on MWCNTs/PDMS composites. To solve agglomeration of MWCNTs in PDMS, dispersant of THF was added, and the resistance of the obtained MWCNTs/PDMS conductive unit with 7.5wt.% MWCNTs was as low as $180\ \Omega$. Meanwhile, high sensitivity ($0.4\ kPa^{-1}$), excellent response stability, fast response time (36 ms) and excellent mechinal-electro properties were demonstrated within pressure range from 0 to 100 kPa. To verify its applicability, a large-area flexible sensor with 8×10 pixels was successfully adopted to detect pressure distribution on the human back. Combining the sensor array with deep learning, inclination of human sitting could be easily recognized with high accuracy, indicating that the combined technology can be used to guide ergonomic design.

Keywords: A. Polymer-matrix composites (PMCs); A. Smart materials; B. Electrical properties; B. Mechanical properties

1. Introduction

With the rapid development of functional materials, integration technology and sensing principles, flexible sensors have recently been widely used in fields of, such as healthcare monitoring, biomedicine, human-machine interaction, *etc.* [1] High sensitivity, long-term stability, and appropriate stretchability are the fundamental characteristics for flexible sensors to mimic human haptic perception. Till now, great progress has been achieved for electronic skin-like flexible pressure sensors, and the design of the pressure sensors is mainly based on one or more of resistive [2-5], piezoelectric [6], capacitive [7] and optical [8] mechanism. Among them, resistive mechanism is widely used to construct flexible pressure sensors due to its simple configuration, wide detection range and high detection accuracy.

Resistive pressure sensors with similar human-skin haptic properties are usually attached to a special part of the human body to monitor physiological signals [9-11] or to a robot to simulate the human body's perception function [12], but they are rarely used to evaluate comfort and guide the ergonomic design of products and parts (e.g. sofas, car seats, mattresses and office chairs) that come in contact with the human body during daily use. It is because that (1) it is still a challenge to make a large-area pressure sensor with uniform structure and performance, and (2) complex circuit and the

resulting signal crosstalk between sensing units greatly reduce the practicability of a large-area pressure sensor. Meanwhile, traditional mechanical sensors which are made of rigid bulk metal usually just have a single-point sensing ability, obviously not satisfying the characteristics of flexibility, conformity, and large-area use. Therefore, a lot of work on comfort evaluation and ergonomic design were carried out based on finite element simulation and subjective evaluation by volunteers, but lack of reliable objective data. As breakthrough works, Reiko *et al.* [13] used a commercial large-area pressure sensor mat to acquire pressure signals on the driver's back and buttocks under various sitting conditions, and analyzed the optimal sitting conditions with a supervised neural network. Ming *et al.* [14] used a large-area thin-film sensors to capture the pressure between the driver and the car seat during driving, by combining with machine learning techniques, the driver's driving posture could be analyzed in real time. Sang *et al.* [15] fabricated 1D/2D heterogeneous composites by dopant-induced composite of 2D $Ti_3C_2T_x$ MXene with 1D nitrogen-doped graphene nanoribbons. The heterogeneous composites were utilized for piezoresistive pressure sensors with noticeably low hysteresis of 1.33% and a wide sensing range (3 Pa-100 kPa). Besides, the heterogeneous composites could be fabricated into a large-area pressure sensor by a scalable solution process,

1
2
3
4
5
6
7
8
9
10
11
12
13
14
15
16
17
18
19
20
21
22
23
24
25
26
27
28
29
30
31
32
33
34
35
36
37
38
39
40
41
42
43
44
45
46
47
48
49
50
51
52
53
54
55
56
57
58
59
60

combining with machine learning algorithms, different sitting posture could be distinguished. All the above-mentioned work was carried out based on thin film pressure sensors which fabrication required expensive equipment and sophisticated integration technology, and the resulting expensive costs limit their wide applicability.

Here, we propose a resistive pressure sensor array that is easy to manufacture and its circuit layout can be freely integrated. The substrate circuit for each sensing unit is independent which avoids the problems of signal crosstalk and endows the sensor layout with strong design freedom. The resistive pressure sensor unit is made of carbon nanotubes (MWCNTs)-PDMS composites. CNTs have been becoming the most commonly used conductive materials because of its favorable mechanical and electrical properties [16-18]. Rekha *et al.* [19] developed a CNTs-based piezoresistive flexible pressure sensor with a square tab diaphragm structure for biomedical applications, which was able to detect pressure as low as 0-5 kPa with higher sensitivity and linearity. Li *et al.* [20] presented a high-sensitivity flexible haptic sensor based on MWCNTs arrays with cross-contact electrodes patterned. The isotropic microstructure provided the sensors with ultra-high sensitivity (-9.95 kPa^{-1}) at low pressure level below 100 Pa, and also excellent stability and fast response time (<200 ms). Obviously, CNTs-elastomer

composites have superior piezoresistive properties, and by altering the spatial structure or the ratio of CNTs in elastomer, the obtained composites are able to detect various pressure ranges, and therefore competent to evaluate comfort and guide the ergonomic design of daily products and parts.

In this work, we design and demonstrate a resistive flexible pressure sensor array based on MWCNTs/PDMS composites with the characteristics of simple manufacturing, low cost, and adjustable circuit layout. The prepared sensors show an ultra-high sensitivity (0.4 kPa^{-1}) and fast response time (~36 ms) at pressure below 100 kPa. Importantly, the independence of sensing units solves the problem of signal crosstalk in large-area pressure sensors, and the measured electrical signals are accurate enough to be used to evaluate comfort and guide ergonomic design. As a demonstration, a large-area 8×10 pressure sensing array was used to collection the pressure distribution in the contact area between the human body and the backrest with different inclination angles. By combining with deep learning technology, a driver' driving behavior can be recognized with an accuracy >94%, indicating the great application potentials in areas such as motion detection, human-machine interaction and wearable devices.

2. Experiment section

2.1 Materials and chemicals

1
2
3 Multi-walled carbon nanotubes
4 (MWCNTs) with a length of 15-20 μm and a
5 diameter of 5-10 nm were purchased from
6 Jiangsu Xianfeng Nano Company (China).
7 Before use, the MWCNTs were carboxylated
8 in 70% nitric acid to enhance the
9 dispersibility in PDMS[21]. Ausbond 529
10 epoxy conductive adhesive was purchased
11 from Shenzhen Ausbond Co., Ltd., China.
12 Polyethylene terephthalate (PET) with a
13 thickness of 0.125 mm (Fellowes Inc., USA),
14 PDMS (Slygard 184 Silicone Elastomer Kit,
15 Dow Corning Corporation), conductive
16 silver ink (DJ912, Shenzhen Welsolo
17 Electronic Technology Co., Ltd., China),
18 tetrahydrofuran (THF), hydrochloric acid
19 (HCl) and nitric acid (HNO_3) (Sigma-
20 Aldrich, China) were used as received
21 without any pre-treatment.

2.2 Functionalization of MWCNTs

35
36 Before functionalization, commercial
37 MWCNTs were first purified by acid
38 washing and drying steps. Specifically, 50
39 mg of MWCNTs was refluxed in 100 mL of
40 35%-37% HCl while being magnetically
41 stirred at 500 rpm for 24 h. To collect
42 MWCNTs, final mixture was centrifuged at
43 9,000 rpm, followed by washing with
44 deionized water until neutralized. MWCNTs
45 were dried in oven for 12 h at 100 °C. To
46 improve the dispersion rate of the purified
47 MWCNTs, MWCNTs were functionalized
48 with carboxylic groups (-COOH). 500 mg of
49 MWCNTs were suspended in 30 mL 70%
50 HNO_3 and then sonicated for 1 h at 60 °C. To

51 collect the functionalized MWCNTs, the
52 mixture was centrifuged followed by
53 washing with deionized water until
54 neutralized. Functionalized MWCNTs were
55 obtained by drying in oven for 12 h at 100 °C.
56 The functionalized MWCNTs were used to
57 fabricate MWCNTs/PDMS composites by a
58 solution mixing and post-curing procedure.

2.3 Fabrication of MWCNTs/PDMS pressure sensitive units

59 The pressure sensitive units with
60 different mass ratio of MWCNTs to PDMS
61 (5.0%, 7.5% and 10.0%) were prepared by
62 solution mixing and post-curing method. To
63 improve the dispersibility of MWCNTs in
64 PDMS, MWCNTs and PDMS were first
65 mixed well with 0.1 mg mL⁻¹ THF,
66 respectively. And then, the above two
67 solutions were mixed and magnetically
68 stirred in a 80 °C water bath for THF
69 evaporation. After 1 h, curing agent (cure :
70 base=1 : 10) was added to the mixer, stirred
71 vigorously for 10 min, and then poured into
72 hemispherical PTFE template. Repeated
73 vacuuming and air intake were carried out to
74 eliminate air bubbles inside the composite,
75 final MWCNTs/PDMS pressure sensitive
76 units were obtained after curing at 60 °C for
77 2 h.

2.4 Preparation of electrode film

78 PET film with a thickness of 0.125 mm
79 in thickness was used as a transparent and
80 flexible substrate material; a commercial
81 silver nanoparticles (Ag NPs) ink was used

to prepare the conductive electrode. The electrode film was fabricated using an inkjet printer (Scientific3, China). Before printing, pre-drawn electrode pattern file was imported into the inkjet printer software. And then the Ag NPs ink was injected into the print cartridge; a nozzle with a proper diameter was selected to ensure a uniform ink output, and the printing parameters were set. Detailed printing parameters can be seen in [Table S1](#) in supporting information. After sintering at 130 °C for 30 min, the high-resolution Ag/PET electrode film was obtained as shown in [is shown Fig. S1](#) in supporting information.

2.5 The assembly of sensor arrays

Due to the poor adhesion between PDMS-based materials and other substrate materials, we used the elastic epoxy-based conductive adhesive Ausbond 529 to bond the MWCNTs/PDMS pressure sensitive units with Ag/PET film. Firstly, two components of A and B of Ausbond conductive adhesive were mixed in the mass ratio of 1 : 1, and then the mixture was evenly smeared onto the lower surface of the MWCNTs/PDMS hemispheres which were then placed onto the appropriate position of the Ag/PET films. A large-area pressure sensing array ([Fig. S2](#) in supporting information) was obtained after heating at 60 °C for 2 h.

2.6 Characteristics

The micromorphology of the fabricated MWCNTs/PDMS composites was

characterized using an ultra-high resolution field emission scanning electron microscope (Verios G4 Thermo Fisher USA) with a CCD camera module. The mechanical-electro properties of the fabricated MWCNTs/PDMS composites with different contents of MWCNTs were investigated by a combined use of a universal materials testing machine (UMT, USA) and a digital multimeter (DMM6500 Keithley, USA). Kickstartfl-suite software was employed to analyze the piezoresistive characteristics of the MWCNTs/PDMS pressure sensitive units and the pressure sensor arrays.

2.7 Design of deep neural network for classification

Convolutional neural networks (CNNs [22]) were applied to class the human sitting behavior based on the pressure distribution collected by large-area MWCNTs/PDMS sensing array ([Fig. 1a](#)). Specifically, a large-area 8 × 10 pressure sensing array was fixed on a seat backrest. The back contact pressure was recorded under the conditions of backrest tilts ranging from 95–115° ([Fig. 1b](#)) using a real-time signal acquisition system ([Fig. 1c](#)). The schematic illustration of signal acquisition circuit is shown in [Fig. S3](#) in supporting information. For sitting behavior classification of smart seat backrest, a total of 200 input data (vector) was generated for the five sitting behavior (100 iterations per item). In the training data preprocessing stage, Gaussian filtered was utilized for noise removal, and z-score normalized was also

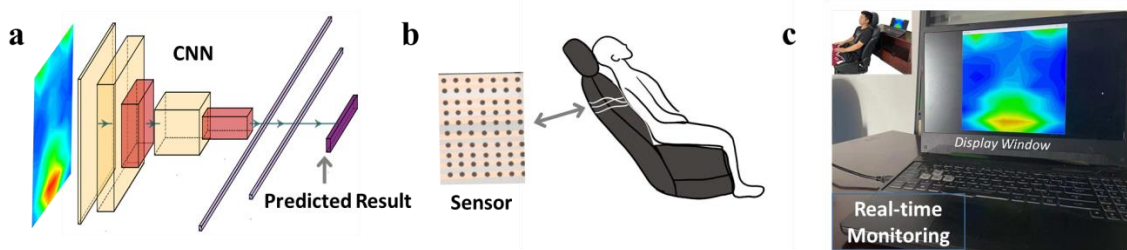


Fig. 1. Machine-learning-assisted sitting behavior recognition. (a) The basic framework of CNN. (b) Schematic illustrating the large-Area sensing array attached on a seat backrest. (c) Image showing the data acquisition and visualization system.

applied. We divided the data into training sets and validation sets in a ratio of 3:1. The detailed description of CNNs training workflow is represented in the supporting information of Fig. S4.

2D CNN algorithm was applied for sitting behavior classification based on pressure distribution. Our neural network consisted of two parts: feature extractor and classifier. Feature extractor was mainly composed of 5 convolution layers and 2 pooling layers. The convolutional layers extracted semantic characteristics via 3×3 filters and generated a new feature map. The pooling layers were used for reduce map

resolution and enlarge the receptive field, which could help network to capture global information. In addition, feature map of every convolutional operation was fed into batch normalization (BN) and was activated by ReLU function. Classifier consisted of 3 dense layers and Soft-max function. Dense layers worked as the connection of final output with the extractor, and Soft-max function was applied for generate the prediction probability of multi-class task. Considering the problems related to learning efficiencies, overfitting, and vanishing gradient, dropout with a rate of 0.5 was also utilized after the front two dense layers.

integrating the sensing units to solve the above-mentioned issues. A scheme illustrating the fabrication procedure of the large-area MWCNTs/PDMS pressure sensing array is presented in Fig. 2. Detailed description is given in the Experiment section in this paper. In brief, before mixing carboxyl-MWCNTs with PDMS, the two materials were uniformly mixed with a certain amount of THF to improve the dispersibility of the carboxyl-MWCNTs in the PDMS and solve the agglomeration

3. Results and Discussion

3.1 Fabrication of large-scale flexible pressure sensing arrays

The preparation of large-area pressure sensors and the signal crosstalk between sensing units have always been key issues restricting their practical applications. Here, we propose a strategy of designing an independent sensing circuit and manually

problem [23]. The resulting mixture was continuously stirred and sonicated until uniformly mixed, transferred to a pre-fabricated PTFE template, and then cured at 60 °C for 2 h to obtain the MWCNTs/PDMS pressure sensing units. Meanwhile, Ag/PET electrode film was fabricated by inkjet

Fig. 3 shows the SEM images of the MWCNTs/PDMS composites with different MWCNTs contents (5.0wt.%, 7.5 wt.% and 10.0 wt.%). It shows that MWCNTs are evenly dispersed in the PDMS substrate and no obvious agglomeration can be observed. This is quite essential for the fabrication of large-area pressure sensing arrays with uniform performance. As proposed by previous researchers [14-25], the conductive mechanism of MWCNTs-polymer composites is based on two major approaches: (1) the interconnection of CNTs to form a conductive network, and (2) the quantum

tunneling effect induced by the dense distribution of CNTs carbon tubes within composites. The minimum MWCNTs content of the PDMS conductive units prepared in this experiment is 5%, and in the SEM images, it can be observed that the cluster spacing between the carbon nanotubes within composites with three MWCNTs contents is less than 0.5 μm, and the adjacent carbon nanotubes are completely connected to form a conducting network, thus, it also shows that the three fabricated MWCNTs/PDMS conductive units have excellent electrical properties (discussed in detail later).

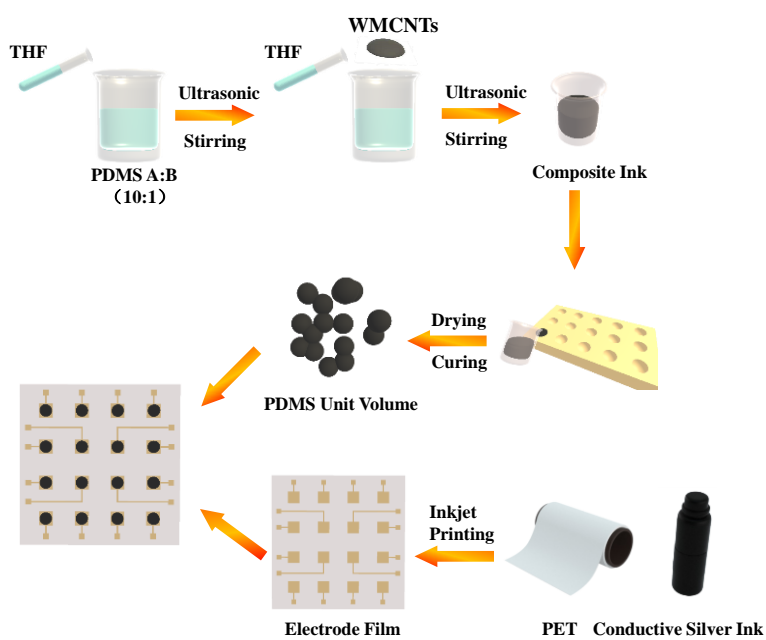


Fig. 2. Scheme of the sample preparation of WMCNTs/PDMS based flexible pressure sensing array.

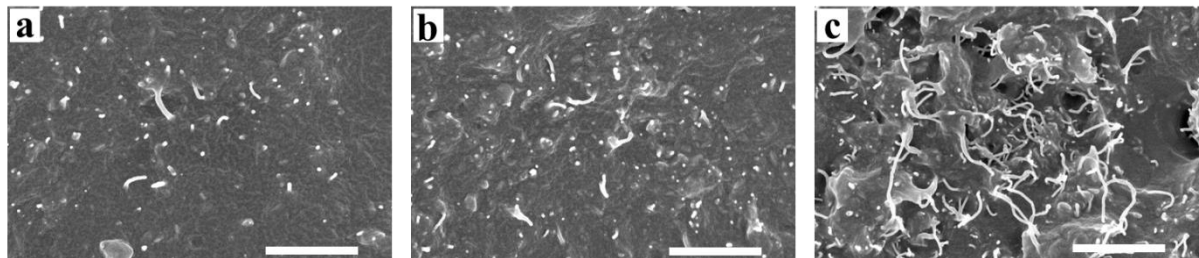


Fig. 3. SEM images of the fabricated MWCNTs/PDMS composites with different MWCNTs contents. (a) 5.0wt.%, (b) 7.5 wt.% and (c) 10.0 wt.%, scale bar=1 μm .

Fig. S1 shows a photograph of the Ag/PET electrode film fabricated by inkjet printing. Metallic luster is observed on the Ag electrode, indicating the composition of metallic silver. The optical microscopic image of the Ag/PET electrode in **Fig. S5** in supporting information shows that a very homogeneous Ag film formed on PET substrate with good quality line features and pattern features. The resistivity of the Ag electrode is $10.0 \pm 0.7 \mu\Omega\cdot\text{cm}$, fully meeting the requirements of good electrical conductivity for the basic circuit. After integrating a MWCNTs/PDMS hemisphere with the Ag/PET basic circuit, a sensing unit is fabricated which can serve as a conductive path to light up a LED bulb with a 3 V DC power supply (**Fig. S6** in supporting information). But under compressed state, the LED bulb turn dark, indicating that the sensing unit can sensitively detect external pressure and the overall device is mechanical robust.

3.2 Mechanical property and linear response behavior

The static stability of the pressure-sensitive unit affects the immunity of the

pressure sensors composed of it to a certain extent. To investigate the static stability of the MWCNTs/PDMS pressure sensitive units with different MWCNTs contents, the electrical resistance of the pressure sensitive units was measured using a Keithley DMM6500 multimeter under non-loading condition. The I - V curves in **Fig. 4a** show that the resistance value of the MWCNTs/PDMS pressure sensitive units changes greatly as the MWCNTs content increases. When the MWCNTs content increases from 5.0 wt.% to 10.0wt.%, the resistance value of the prepared MWCNTs/PDMS units sharply decreases by about 167 times, from $30 \text{ k}\Omega$ to about 180Ω , which is consistent with the results reported in previous publication [24]. This is due to the fact that variation in the MWCNTs content leads to the difference in the density of the conductive network formed inside the fabricated conductive composites. As the content of MWCNTs increases, the density of the conductive network increases, so the electrical performance of the prepared MWCNTs/PDMS pressure-sensitive unit also improves. In addition, it can also be observed from the I - V curves that the resistance values of the MWCNTs/PDMS

pressure sensitive units with different MWCNTs contents is very stable, and hardly affected by the voltage applied, which should be attributed to the point that even the MWCNTs/PDMS conductive unit with only 5.0 wt.% MWCNTs content has exceeded the threshold upper limit of percolation theory [28, 29] and thus the conductive unit as a whole presents the characteristics of a resistive element. The MWCNTs/PDMS conductive units were designed as a hemisphere to increase deformability and consequently improving the pressure-sensing sensitivity, calculated as $S=\Delta R/(R_0 \times P)$, where $\Delta R/R_0$ is the relative resistance change, P is the applied pressure in the range of 0-120 kPa. Fig. 4b shows that the conductive units with different MWCNTs contents have different pressure sensing capabilities, and high MWCNTs content determines good pressure sensitivity but narrow pressure-sensitive range. The sensitivity of the MWCNTs/PDMS units is 0.24 kPa^{-1} in $0-88\pm 2\text{ kPa}$, 0.40 kPa^{-1} in $0-103\pm 2\text{ kPa}$ and 0.45 kPa^{-1} in $0-120\text{ kPa}$ for 5.0 wt.%, 7.5 wt.% and 10.0 wt.% MWCNTs contents, respectively. Moreover, within pressure-sensitive range, the sensitivity for each conductive unit increases linearly with the increase of pressure. However, further increasing applied pressure to 120 kPa will cause the sensitivity of different sensing units to show different trends, and the sensitivity of the MWCNTs/PDMS conductive unit with 5.0% MWCNTs is almost unchanged, while

the other two are significantly reduced. This is because when the internal conductive path of the composites is not saturated, the higher the initial MWCNTs content within the composite, the more new conductive paths are formed in the composite when small pressure is applied, and the more obviously the resistance decreases. Consequently, the sensitivity of this sample presents greater. When the external pressure is large enough, the internal conductive path of the composite with high MWCNTs content is dense enough, or even saturated. At this time, continuous applying external pressure plays little effect on its conductivity, so the sensitivity significantly reduces. It is conceivable that the higher the content of MWCNTs in the composite, the earlier it will reach a stable conductive state, and thereby its pressure-sensitive range will be smaller than that of the samples with low content of MWCNTs.

The compression behavior and the calculated compressive elastic modulus are presented in Fig. S7 in supporting information and Fig. 4c, respectively. The compressive elastic modulus for MWCNTs/PDMS composites with 5.0wt.%, 7.5 wt.% and 10.0 wt.% MWCNTs contents is $2.34\pm 0.3\text{ MPa}$, $3.71\pm 0.4\text{ MPa}$ and $5.00\pm 0.2\text{ MPa}$, respectively. Comprehensive consideration of the electrical conductivity and mechanical properties of the composites, the MWCNTs/PDMS composite with 7.5wt.% MWCNTs is more suitable for preparing large-area pressure sensors, and its pressure

sensing performance is further investigated. The stress-strain curves in Fig. 4d(i) shows 7.5wt.% MWCNTs/PDMS composite exhibits fully elastic after 50 cycles of

compression (strain=10%) and release (strain=0%), and during the cyclic compression process, the change trend of $\Delta R/R_0$ shown in Fig. 4d(ii) is highly

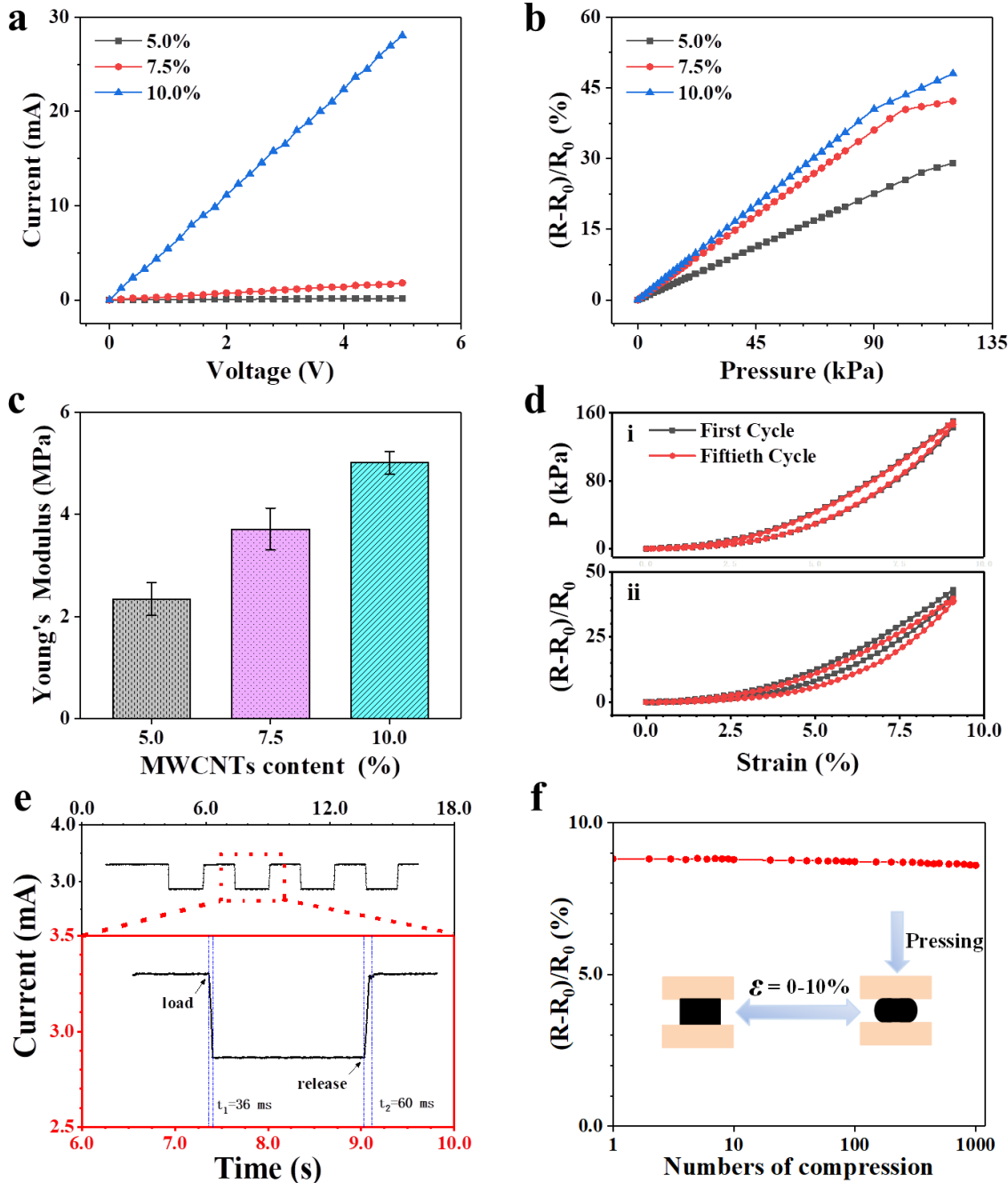


Fig. 4. Mechanical-electro properties of MWCNTs/PDMS sensing unit. (a) $I-V$ characteristics of MWCNTs/PDMS composites with WMCNTs contents of 5.0wt.%, 7.5 wt.% and 10.0 wt.%. (b) Resistance change over pressures for MWCNTs/PDMS composites. (c) Young's modulus of MWCNTs/PDMS composites. (d) Simultaneously cyclic compression stress-strain and resistance change curves for 7.5 wt.% MWCNTs/PDMS composite. (e) Current response of the MWCNTs/PDMS pressure sensing unit during a press and release process. (f) Cyclic stability of the MWCNTs/PDMS pressure sensing unit.

consistent with that of stress with strain. No obvious hysteresis can be observed. Besides, 7.5wt.% MWCNTs/PDMS sensing unit can make a rapid response to external pressure. As shown in Fig. 4e, when there is no external pressure, the current value stabilizes at 3.3 mA. Once a external pressure of 50 kPa is applied, the current quickly decreases to 2.86 mA, and then stabilizes. This process demonstrates that the MWCNTs/PDMS sensing unit can quickly respond to external pressure, and the response time to pressure loading and unloading is 36 ms and 60 ms, respectively. Finally, the stability of MWCNTs/PDMS sensing unit was investigated by continuously monitoring the resistance change of the sensing unit during 1000 cycles of compression to stain of 10%.

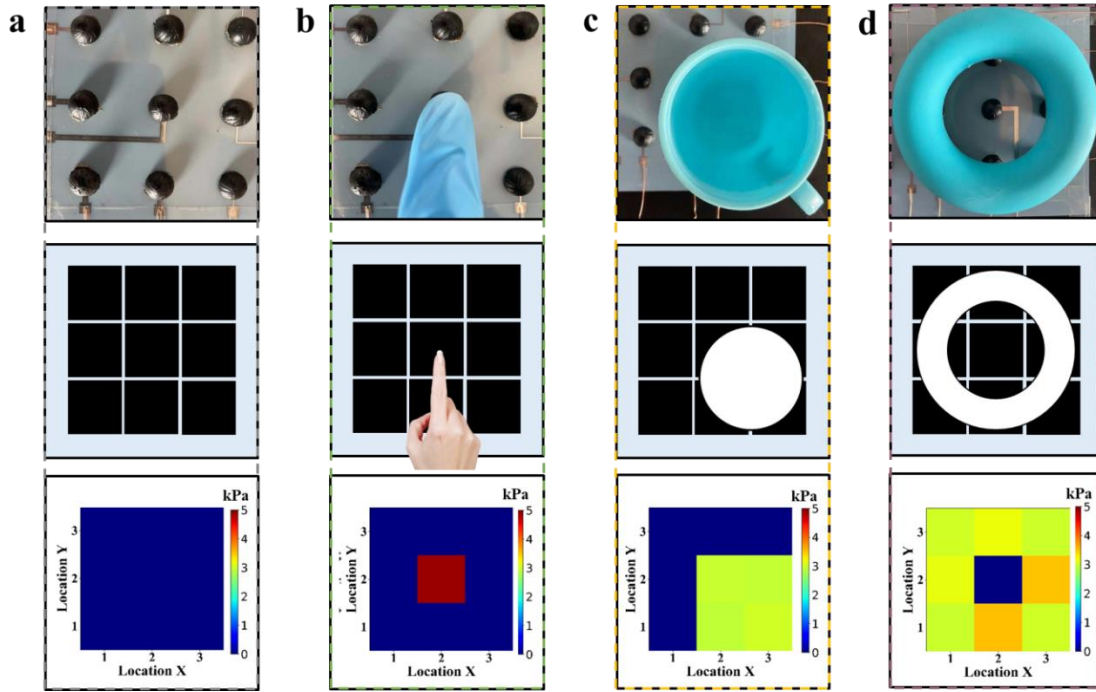


Fig. 5. Pressure sensing performance of a 3×3 MWCNTs/PDMS sensing array. Images of a 3×3 MWCNTs/PDMS sensing arrays (top), schematic of the sensing arrays (middle) and corresponding output images (bottom) under the conditions of (a) no pressing and pressing with (b) a single finger, (c) a cup of water, and (d) a rubber ring.

Fig. 4f shows after 1000 cycles of compression, the resistance only changes by 2.3%, proving that the stability of the MWCNTs/PDMS is good to meet the needs of the application.

To demonstrate our idea that free assembly circuit can reduce signal crosstalk and increase circuit designability, we integrated a 3×3 sensing array to exam its pressure detecting and imaging ability. Fig. 5a shows that separate wires were attached to the data collecting and processing system for each sensing pixel to avoid interference between measured signal. When an object was placed on the pressure sensing array, the data processing system would automatically record the resistance change at the pressure-bearing pixel, and show it in different

1
2
3 colors. Fig. 5b-d demonstrates the pressure
4 sensing array can easily detect the pressure
5 values and distribution positions of fingers,
6 cups and rubber rings. The pressure value of
7 the pixel where there is no object contact is
8 displayed as 0 kPa, and the pixel where there
9 is an object contact can accurately detect the
10 pressure that it bears. More importantly, no
11 matter how much pressure a pixel bears, its
12 adjacent pixels are not disturbed. The above
13 research proves the feasibility of our idea and
14 shows that based on this idea, we can
15 integrate a large-area pressure sensor to
16 evaluate comfort and guide ergonomic
17 design of products and parts.
18
19
20
21
22
23
24
25
26
27
28
29

3.3 Sitting behavior recognition

30 In view of the characteristics of the
31 MWCNTs/PDMS sensor, such as high
32 sensitivity, fast response time, good
33 flexibility, accurate data, and strong circuit
34 layout design, we prepared a large-area
35 sensor of 8×10 pixels to measure the pressure
36 distribution of the human back on the
37 backrest of a car seat. 40 male volunteers
38 with a height of 170 ± 2 cm and a weight of
39 70 ± 2 kg participated in the test. As shown in
40 Fig. 6a, the volunteer's back was in natural
41 contact with the backrest adjusted to different
42 inclination angles from 95° to 115° , and each
43 increase of 5° was a tested condition to
44 simulate and study the sitting behavior and
45 its influence on the human back pressure
46 distribution during driving. As we all know,
47
48
49
50
51
52
53
54
55
56
57
58
59
60

excessive forward or backward leaning
during driving will cause skeletal and muscle
compensatory behavior, making the driver
prone to fatigue and even causing spinal
problems. Undoubtedly, reasonable sitting
behavior and comfortable seat design will
solve the above problems. To efficiently and
accurately judge the degree of pressure on the
human back in different sitting positions, a
typical machine learning model CNN was
used, which mimic human cognitive
processes and have the ability to learn and
represent complex data [30,31]. Fig. 6a
shows that during CNN training process, the
accuracy of the training sets and the
validation sets increases with the number of
iterations, and convergence is achieved when
the epoch reaches about 60. The confusion
matrix obtained by comparing the prediction
results with the labels shows that the 2D
CNN algorithm can accurately identify five
kinds of human sitting behavior with an
accuracy rate of 0.94, 0.96, 0.98, 0.98 and
0.98, respectively (Fig. 6b). The receiver
operating characteristic (ROC) in Fig. 6c
indicates our method can also achieve a high
true positive rate (TPR) as well as a low false
positive rate (FPR), further demonstrating
that the 2D CNN algorithm has high
classification accuracy. As a result, the
combine of the CNN algorithm with a large-
area pressure sensor can efficiently and
accurately recognize a person's sitting
behavior as shown in Fig. 6d.

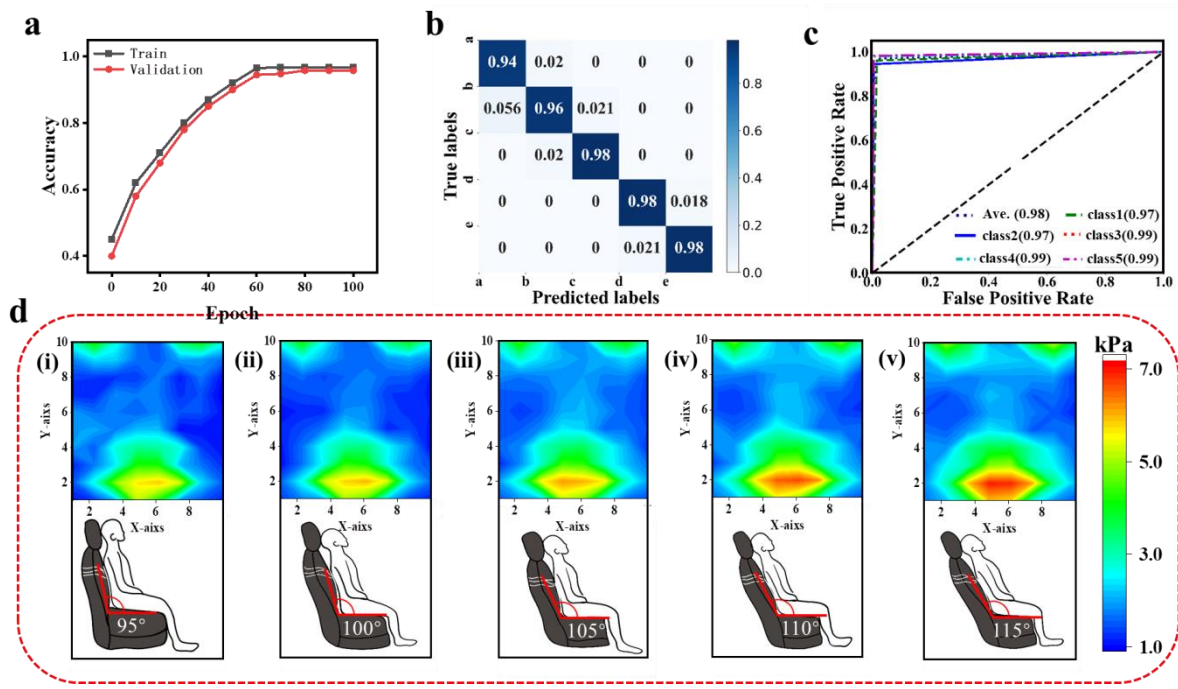


Fig. 6. Large area flexible sensor combined with neural network for sitting posture discrimination (a). The train accuracy and validation accuracy from different epoch (b). The confuse matrix of various categories (c). The receiver operating characteristic (ROC) of various categories (d). Five types of sitting postures and the corresponding pressure clouds

4. Conclusion

In summary, we developed a simple method to fabricate haptic pressure-sensitive units based on MWCNTs/PDMS composites. The sensing units exhibit a combined performance of high sensitivity (<100 kPa, $S \approx 0.4$ kPa $^{-1}$), outstanding response stability, fast response time (36 ms), long-term signal stability, and excellent force-electric synchronization. The sensing units can be integrated into a large-area sensing array with any layout because the substrate circuit for each sensing unit is independently designed, which avoids the problems of signal crosstalk and endows the sensor layout with strong design freedom. The large-area MWCNTs/PDMS sensing array shows

excellent signal detection capability. Combined with deep learning, inclination of human sitting could be easily recognized with high accuracy, indicating that the combined technology can be used wearable devices to guide ergonomic design.

Supporting information

Photographs of the Ag/PET electrode film and the large-area pressure sensing arrays; Scheme of the signal collection circuit; The workflow of CNNs training stage; Optical microscopic images of the Ag/PET electrode; The change in brightness of a LED bulb showing the pressure-sensitive of MWCNTs/PDMS composite unit; Compressive stress-strain curve of WMCNTs/PDMS samples with different WMCNTs contents; Table listing detailed parameter setting for microelectronic printing.

Conflict of interest

The authors declare no conflict of interest.

Acknowledgments

This work was supported by the National Natural Science Foundation of China (Grant No. 52103025) and the Education Scientific Research Project of Young Teachers in Fujian Province (Grant No. JA15306).

References

- [1] Khoshbin Z, Housaindokht M R, Izadyar M, et al. Recent advances in computational methods for biosensor design. *Biotechnol Bioeng.*, 2021, 118(2): 555-578.
- [2] Takahashi T, Takei K, Gillies A G, et al. Carbon nanotube active-matrix backplanes for conformal electronics and sensors. *Nano Lett.*, 2011, 11(12): 5408-5413.
- [3] Gong S, Schwalb W, Wang Y, et al. A wearable and highly sensitive pressure sensor with ultrathin gold nanowires. *Nat Commun.*, 2014, 5(1): 1-8.
- [4] Xie X, Huang H, Zhu J, et al. A spirally layered carbon nanotube-graphene/polyurethane composite yarn for highly sensitive and stretchable strain sensor. *Compos. Part. A-Appl. S.*, 2020, 135: 105932.
- [5] Aly K, Li A, Bradford P D. Strain sensing in composites using aligned carbon nanotube sheets embedded in the interlaminar region. *Compos. Part. A-Appl. S.*, 2016, 90: 536-548.
- [6] Persano L, Dagdeviren C, Su Y, et al. High performance piezoelectric devices based on aligned arrays of nanofibers of poly(vinylidenefluoride-co-trifluoroethylene). *Nat. Commun.*, 2013, 4(1): 1-10.
- [7] Lipomi D J, Vosgueritchian M, Tee B C K, et al. Skin-like pressure and strain sensors based on transparent elastic films of carbon nanotubes. *Nat. Nanotechnol.*, 2011, 6(12): 788-792.
- [8] Yilmazoglu O, Popp A, Pavlidis D, et al. Vertically aligned multiwalled carbon nanotubes for pressure, tactile and vibration sensing. *Nat. Nanotechnol.*, 2012, 23(8): 085501.
- [9] Huang Y, Zhang J, Pu J, et al. Resistive pressure sensor for high-sensitivity e-skin based on porous sponge dip-coated CB/MWCNTs/SR conductive composites. *Mater. Res. Express*, 2018, 5(6): 065701.
- [10] Tannarana M, Solanki G K, Bhakhar S A, et al. 2D-SnSe₂ nanosheet functionalized piezo-resistive flexible sensor for pressure and human breath monitoring. *ACS. Sustain. Chem. Eng.*, 2020, 8(20): 7741-7749.
- [11] He Y, Zhou Y Y, Liu H. Research progress of flexible pressure sensors based on carbon materials. *Chem. Eng. Prog.*, 2018, 322(07): 215-222.
- [12] Rocha R P, Lopes P A, De Almeida A T, et al. Fabrication and characterization of bending and pressure sensors for a soft prosthetic hand. *J. Micromech. Microeng.*, 2018, 28(3): 034001.
- [13] Mitsuya R, Kato K, Kou N, et al. Analysis of body pressure distribution on car seats by using deep learning. *Appl. Ergon.*, 2019, 75: 283-287.
- [14] Ding M, Suzuki T, Ogasawara T. Estimation of driver's posture using pressure distribution sensors in driving simulator and on-road experiment. 2017 IEEE International Conference on Cyborg and Bionic Systems (CBS). IEEE, 2017: 215-220.
- [15] Lee H J, Yang J C, Choi J, et al. Hetero-Dimensional 2D Ti₃C₂Tx MXene and 1D Graphene Nanoribbon Hybrids for Machine Learning-Assisted Pressure Sensors. *ACS. Nano.*, 2021.
- [16] Lee J H, Rhee K Y, Park S J. Silane modification of carbon nanotubes and its effects on the material properties of carbon/CNT/epoxy three-phase composites. *Compos. Part. A-Appl. S.*, 2011, 42(5): 478-483.

- [17] Nam T H, Goto K, Yamaguchi Y, et al. Effects of CNT diameter on mechanical properties of aligned CNT sheets and composites. *Compos. Part. A-Appl. S.*, 2015, 76: 289-298.
- [18] Ma P C. N. a. Siddiqui, G. Marom, and J.-K. Kim. Dispersion and functionalization of carbon nanotubes for polymer-based nanocomposites: A review. *Compos. Part. A-Appl. S.*, 2010, 41(10): 1345-1367.
- [19] Devi R, Gill S S. A squared bossed diaphragm piezoresistive pressure sensor based on CNTs for low pressure range with enhanced sensitivity. *Microsyst. Technol.*, 2021: 1-9.
- [20] Li X, Huang W, Yao G, et al. Highly sensitive flexible tactile sensors based on microstructured multiwall carbon nanotube arrays. *Scripta. Mater.*, 2017, 129: 61-64.
- [21] Liu Z, Lin X, Lee J Y, et al. Preparation and characterization of platinum-based electrocatalysts on multiwalled carbon nanotubes for proton exchange membrane fuel cells. *Langmuir.*, 2002, 18(10): 4054-4060.]
- [22] Lecun Y, Bottou L. Gradient-based learning applied to document recognition. *P. IEEE*, 1998, 86(11):2278-2324.
- [23] Hassouneh S S, Yu L, Skov A L, et al. Soft and flexible conductive PDMS/MWCNT composites. *J. Appl. Polym. Sci.*, 2017, 134(18).
- [24] Du J, Wang L, Shi Y, et al. Optimized CNT-PDMS flexible composite for attachable health-care device. *Sensors*, 2020, 20(16): 4523.
- [25] Nankali M, Nouri N M, Geran Malek N, et al. Electrical properties of stretchable and skin-mountable PDMS/MWCNT hybrid composite films for flexible strain sensors. *J. Compos. Mater.*, 2019, 53(21): 3047-3060.
- [26] Simmons J G. Generalized formula for the electric tunnel effect between similar electrodes separated by a thin insulating film. *J. Appl. Phys.*, 1963, 34(6): 1793-1803.
- [27] Hu N, Fukunaga H, Atobe S, et al. Piezoresistive strain sensors made from carbon nanotubes based polymer nanocomposites. *Sensors*, 2011, 11(11): 10691-10723.
- [28] Khosla A, Gray B L. Preparation, characterization and micromolding of multi-walled carbon nanotube polydimethylsiloxane conducting nanocomposite polymer. *Mater. Lett.*, 2009, 63(13-14): 1203-1206.
- [29] Last B J, Thouless D J. Percolation theory and electrical conductivity. *Phys. Rev. Lett.* 00, 1971, 27(25): 1719.
- [30] Joachims T. Text categorization with Support Vector Machines: Learning with many relevant features. *Proc. Conference on Machine Learning*. Springer, Berlin, Heidelberg, 1998.
- [31] DE Rumelhart, Hinton G E, Williams R J. Learning Representations by Back Propagating Errors. *Nature*, 1986, 323(6088):533-536.

Supporting Information

Large-area flexible MWCNTs/PDMS pressure sensor for ergonomic design with aid of deep learning

Hongchuan Zhong^{‡a}, Rongda Fu^{‡a}, Nuo Chen^{‡b}, Shiqi Chen^a, Zaiwei Zhou^a, Yue Zhang^{a,c,*}, Xiangyu Yin^{c,d*}, Bingwei He^{a,b}

a. College of Mechanical Engineering and Automation, Fuzhou University, Fuzhou 350108, China

b. Department of Mechanical and Energy Engineering, Southern University of Science and Technology, Shenzhen 518055, China

c. Fujian Engineering Research Center of Joint Intelligent Medical Engineering, Fuzhou 350108, China

d. College of Chemical Engineering, Fuzhou University, Fuzhou 350108, China

‡ Hongchuan Zhong, Rongda Fu and Nuo Chen contributed equally to this work.

*Corresponding authors: Yue Zhang (yuezhang@fzu.edu.cn); Xiangyu Yin (xyin65@fzu.edu.cn)



Fig. S1. Photograph of the Ag/PET electrode film.

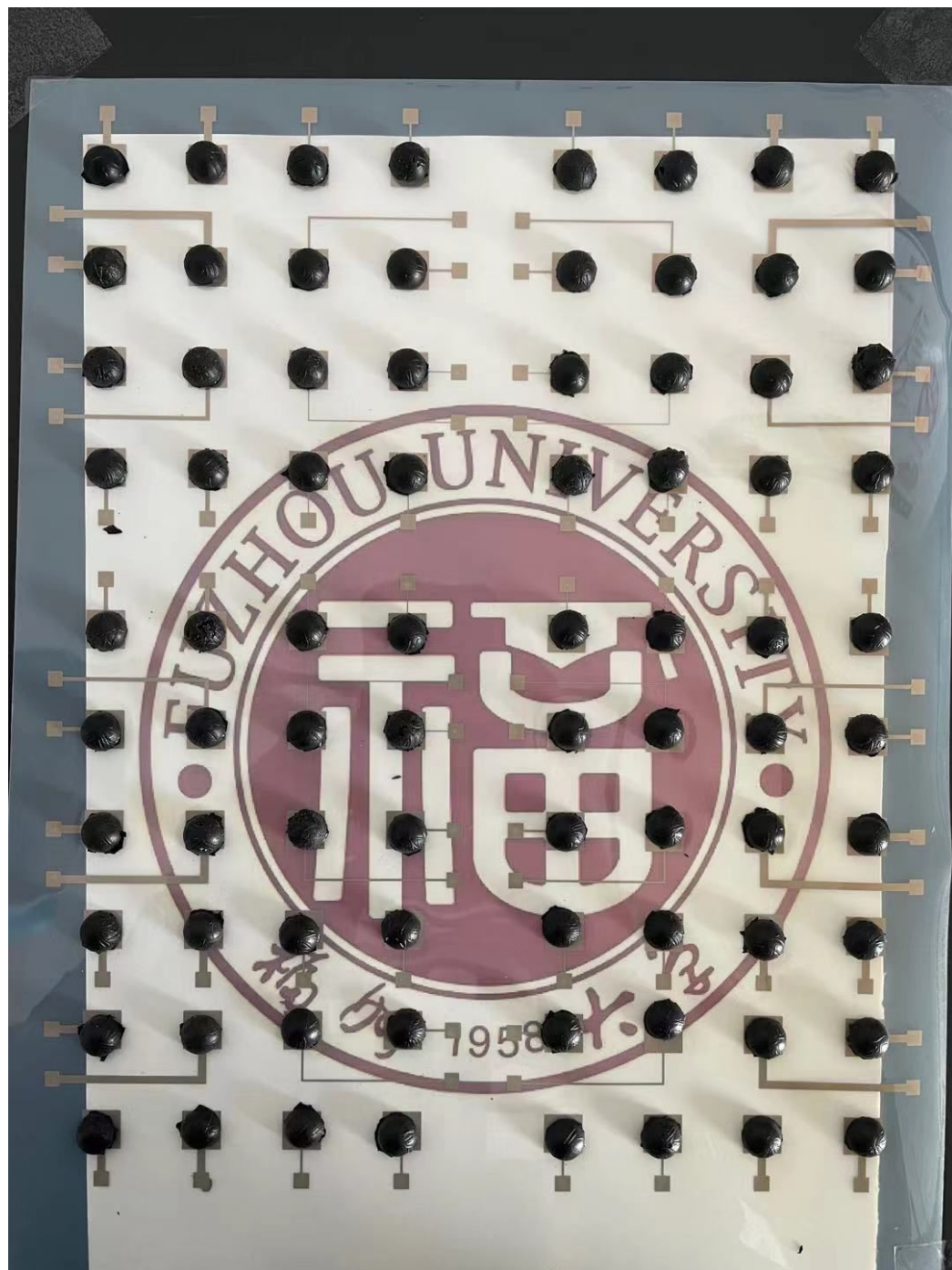


Fig. S2. Photograph of the large-area pressure sensing arrays.

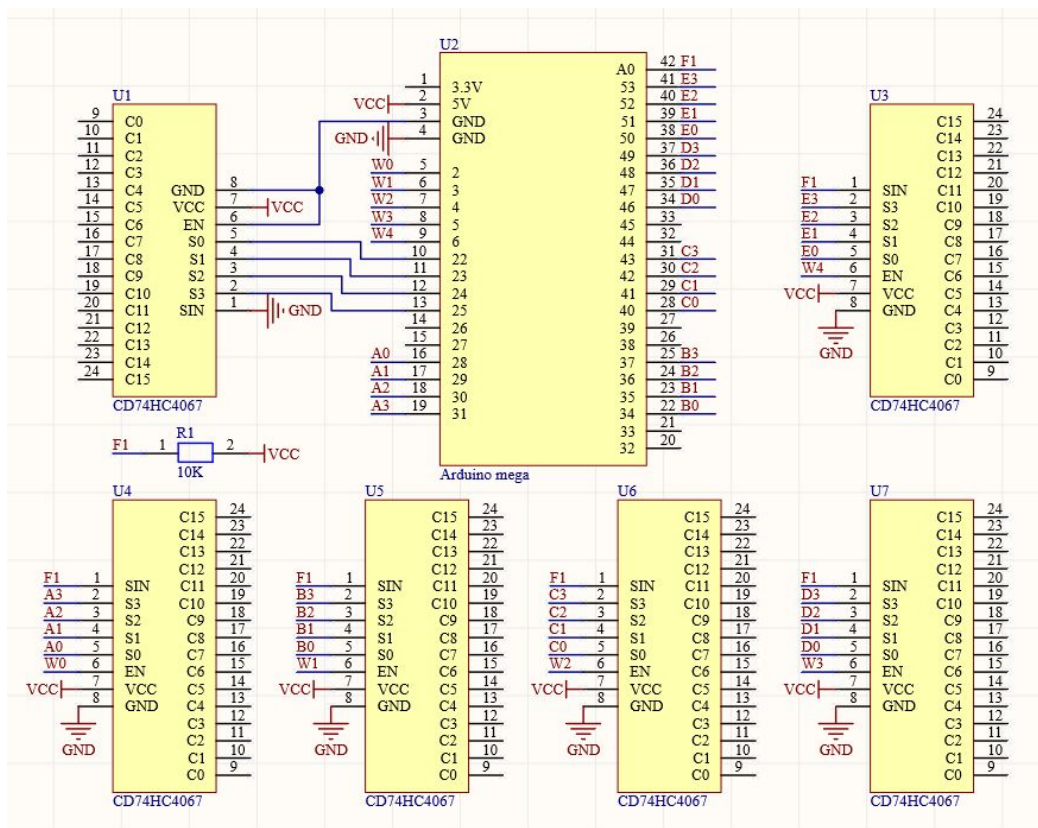


Fig. S3. Scheme of the signal collection circuit.

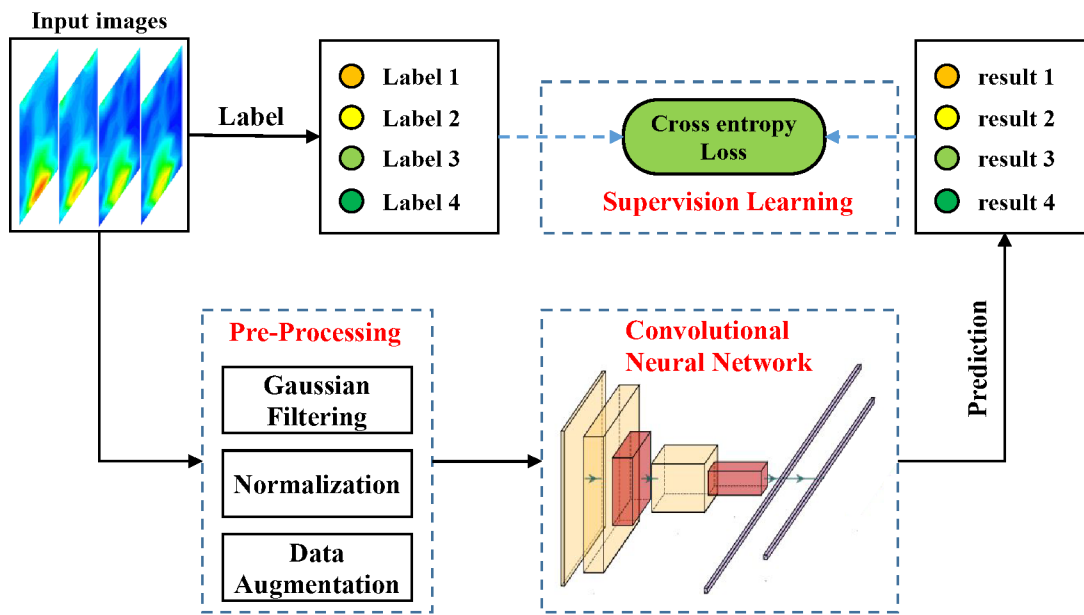


Fig. S4. The workflow of CNNs training stage. The images were smooth with a Gaussian filter and be normalized to [0,1] before training. Data argumentation was applied to avoid over-fitting. Then the training data was fed into CNN and was supervised by the cross-entropy loss function.

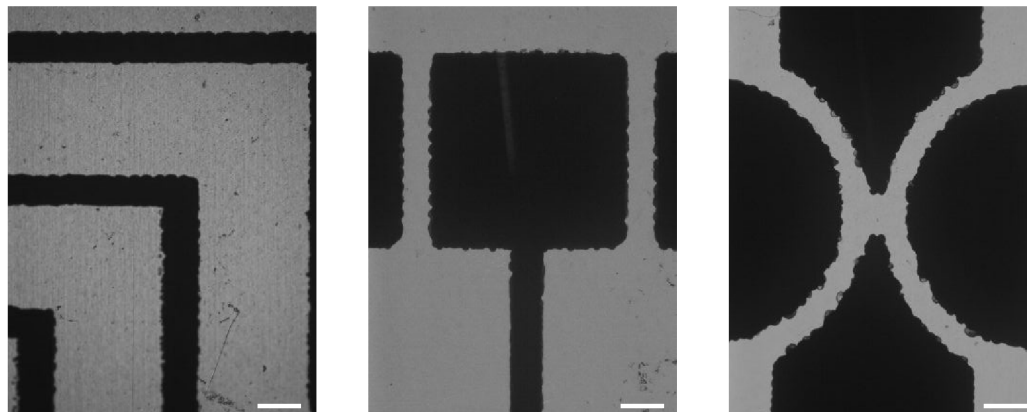


Fig. S5. Optical microscopic images of the Ag/PET electrode (scale bar=250 μm).

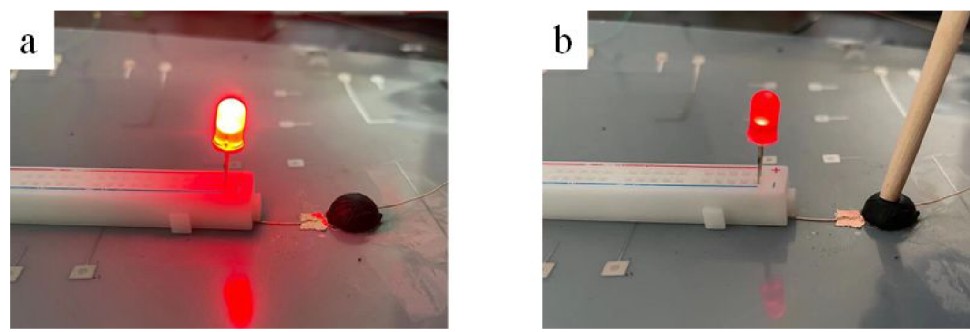


Fig. S6. The change in brightness of a LED bulb showing the pressure-sensitive of MWCNTs/PDMS composite unit.

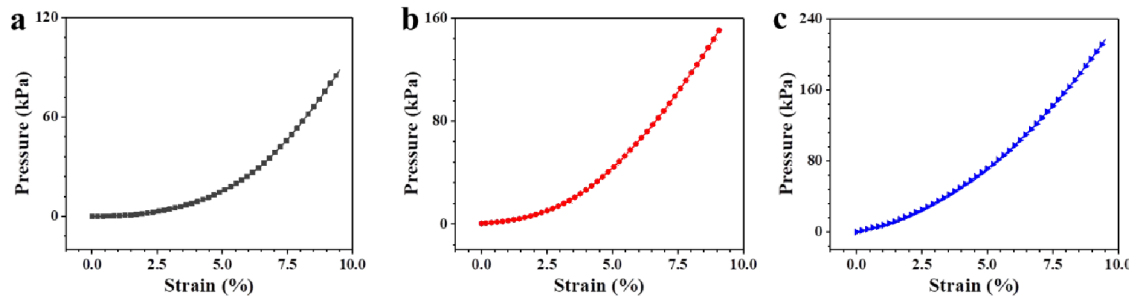


Fig. S7. Compressive stress-strain curve of WMCNTs/PDMS samples with WMCNTs content of (a) 5.0wt.%, (b) 7.5 wt.% and (c) 10.0 wt.%, respectively.

Table S1. Detailed parameter setting for microelectronic printing.

Print settings			Auto clean settings	
Print Pressure	Nozzle Temp	Print Freq/Hz	Clean before printting	Automatic cleaning in printting
-1	0	2000	Uncheck	Uncheck
Cleaning			Cycle	
Times/ms	Cycle/μs	Delay/Sec	Mode	Interval
500	656	0	Round trip	120
Paramenters				
Wave file	Position X/mm	Z up/mm	Z down/mm	Erasure Times
BASE-CP12	2	42	43.5	1